Synchrotron x-ray observation of surface smectic-*I* hexatic layers on smectic-*C* liquid-crystal films

E. B. Sirota, P. S. Pershan, and Suzanne Amador
Physics Department and Division of Applied Sciences, Harvard University, Cambridge, Massachusetts 02138

L. B. Sorensen
Department of Physics, University of Washington, Seattle, Washington 98195
(Received 2 May 1986; revised manuscript received 27 August 1986)

Synchrotron x-ray diffraction methods employing a position-sensitive detector were used to study smectic-*C* (Sm*C*) and smectic-*I* (Sm*I*) phases in thin (2–6 molecular layers) liquid-crystal films of 4-(*n*-heptyloxy)benzylidene-4-(*n*-heptyl)aniline (7O.7). Above ~78 °C, the entire film is Sm*C* and below ~69 °C, the entire film is Sm*I*, a stacked tilted hexatic. Between 69 °C and 78 °C, the surface layers of the films are hexatic Sm*I* and the interior layers are Sm*C*. There is a pretransitional broadening of the surface hexatic peaks as the surface layers melt into the Sm*C* phase.

INTRODUCTION

Recently, considerable theoretical and experimental efforts have been focused on the phase transitions occurring at the surfaces of bulk samples[1] and on the phase transitions in two-dimensional (2D) systems.[2] One of the interesting issues in the surface transition studies involves the influence of the effective surface field generated by the bulk-vacuum interface on the order at the surface. Systems for which surface-field-induced ordering have been studied include liquid metals,[3,4] bulk liquid crystals,[5,6] and smectic liquid-crystal films.[7–10] One of the key unresolved issues in the 2D phase-transition studies involves the behavior of the novel hexatic phases of matter originally predicted by the Kosterlitz-Thouless-Halperin-Nelson-Young (KTHNY) 2D melting theory.[11–13] Experimental studies of the melting transitions in physisorbed monolayers[14] and in freely suspended liquid-crystal films[9,15–17] have demonstrated the existence of hexatic phases of matter in these systems. However, the observed behavior of both these systems is more complicated than that predicted by the original KTHNY melting theory and active theoretical and experimental efforts are continuing.[9,14–17]

In this paper we report the results of the first synchrotron x-ray scattering study demonstrating the existence of surface hexatic smectic-*I* (Sm*I*) layers on the two exterior surfaces of freely suspended smectic-*C* (Sm*C*) liquid-crystalline films. At high temperatures, above ~78 °C, the entire film is Sm*C*; each layer is a tilted two-dimensional liquid. At low temperatures, below ~69 °C, the entire film is Sm*I*; each layer is a tilted two-dimensional hexatic with no observable interlayer coupling. At intermediate temperatures, the two exterior layers are Sm*I* and all of the remaining interior layers are Sm*C*. The analogous formation of surface layers of a low-temperature crystalline-*B* (Cr*B*) phase on the surface of a high-temperature liquid smectic-*A* (Sm*A*) has been reported by Moncton, Pindak, Bishop, and co-workers.[7,8] Taken together, these experiments are important because they clearly indicate the formation of monolayer surface phases produced by the effective surface field. In both of these cases, the melting of the surface phase occurs at a higher temperature than the melting of the corresponding bulk phase indicating a stablization of the ordered phase by the surface field. This observed stabilization is in sharp contrast to the suppression of the melting temperature expected for reduced dimensionality systems [as observed in both the smectic-*F* (Sm*F*) to crystalline-*G* transition[9] and the normal to superfluid transition[18]] and it illustrates the importance of the effective surface field in these systems. The observed melting of the surface crystal layers (Cr*B* on Sm*A*) was first order with no pretransitional effects.[7,8] Because the melting of the tilted hexatic surface phase does not involve a change in symmetry, the only true phase transition must be first order. However, we observed clear pretransitional effects so that the detailed nature of the surface hexatic to tilted liquid transition remains as an intriguing unresolved issue in the behavior of these systems.

The liquid crystal material used in the present study is 4-(*n*-heptyloxy)benzylidene-4-(*n*-heptyl)aniline (7O.7). Previous studies showed that in thin films this material develops tilted hexatic phases (Sm*F* and Sm*I*) which are not found in bulk samples.[9,17] These hexatic phases occur in the temperature range that produces unusual modulated Cr*B* phases in bulk films.[19–22] The origin of these hexatic phases is not understood in detail, but probably involves a lower surface energy for the tilted molecules than for the nontilted molecules. The present study addresses the Sm*C* to Sm*I* transition. At this transition, the in-plane positional correlations grow from the roughly nearest-neighbor correlations found in the Sm*C* phase to correlations over several hundred neighbors found in the Sm*I* phase. In the highly correlated Sm*I* phase, the strong director fluctuations characteristic of the Sm*C* phase are quenched. Visual optical microscopy studies first done by Farber[23] and repeated by one of us (E.B.S.),

identified a transition in thin 7O.7 films at $\sim 78\,^{\circ}C$, where the strong shimmering due to the SmC director fluctuations disappears and is replaced by weakly birefringent domains. It was observed that the domains overlap, suggesting that there are independent domains on the two exterior surfaces. Farber noticed that the texture of the domains for 7O.7 films was different than that expected for the surface crystals, and, based on the x-ray observations[9,17] of hexatic phases in 7O.7, suggested that the 7O.7 surface domains might indicate surface hexatic ordering. Our x-ray scattering studies were undertaken to test this identification.

EXPERIMENTAL RESULTS

The x-ray diffraction studies were carried out on beam line VII-2 at the Stanford Synchrotron Radiation Laboratory (SSRL). A pair of asymmetrically cut Ge[111] crystals were used in the double-crystal monochromator to provide a well-collimated incident beam with $\lambda = 1.577$ Å. Slits located after the monochromator were used to trim the beam to a size of 1mm$\times$4 mm (height$\times$width). A Braun OED-50 position-sensitive proportional counter (PSPC) was used to provide parallel detection of the scattered x-rays. Fig. 1 illustrates the experimental geometry. The active length of the detector is 5 cm; it was oriented normal to the scattered wave vector and in the scattering plane. The detector efficiency is 50% for 8-keV x-rays and the spatial resolution along the detector is 50 microns. When the given resolution is taken into account, the parallel data collection rate was increased by about a factor of 20 over the rate for the conventional nonparallel detector (a LiF analyzer crystal plus scintillation detector). The resolution of the spectrometer was determined by the sample-detector distance (675 mm) and the beam width in the scattering plane (1 mm). Theoretically, this provided a rectangular two-theta resolution function with a full width of $\Delta Q = 4.7\times 10^{-3}$ Å^{-1}. This was confirmed by measurement of the Bragg peaks in the CrB phase at 60 °C. To reduce background scattering into the detector, slits located 545 mm in front of the detector were trimmed to 6 mm in the scattering plane. The trimming also provided a small shadowed portion of the PSPC which was used as a secondary incident beam monitor. The scattered intensity in this portion of the detector was about 0.5 counts per second per mm of the detector and was independent of the film thickness. The χ resolution was fixed by the 1-cm height of the detector and was $\sim 2^{\circ}$ full width at half maximum (FWHM).

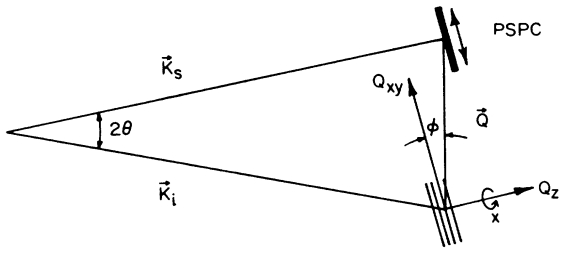

FIG. 1. Schematic illustration of the scattering geometry. The position-sensitive proportional counter (PSPC) is oriented with its active direction perpendicular to the scattering direction and in the scattering plane. Here K_s and K_i are the scattered and incident wave vectors, respectively. Q_{xy} and Q_z are defined the same as in the inset to Fig. 2. The illustrated spectrometer configuration is for a scan that is approximately along Q_{xy} at finite Q_z.

The oven used to produce the freely suspended films has been described elsewhere.[21] The films were oriented with the normal to the smectic layers, $\hat{z}$, in the scattering plane. The angle ϕ between the scattering vector **Q** and the smectic layers could be adjusted to scan different regions in reciprocal space. The configuration illustrated in Fig. 1 corresponds to a finite value of Q_z with the active length of the PSPC nearly parallel to the Q_{xy} direction. For the Q_z direction, the PSPC output typically provides a 2θ scan which makes an angle of approximately 10° to the x-y plane of the smectic layers and is also a good approximation to a Q_{xy} scan. Because of the parallel detection, the Q_z scans normal to the smectic layers could be done with software selectable 2θ resolution by adding together detector channels. The direction of Q_{xy} within the smectic layers was controlled using a χ rotation stage inside the oven.

The structural features of the SmI phase have been studied in some detail.[16,24–27] The molecules are tilted with respect to the smectic layers causing a slight distortion of the quasihexagonal in-plane packing into a monoclinic structure. The packing in the plane perpendicular to the molecules is still nearly hexagonal. The resulting x-ray scattering peaks for the SmI phase are shown in Fig. 2. For the thin 7O.7 films used in this study, the samples consisted of many small in-plane domains resulting in scattering patterns which were powder averaged over χ. The resulting powder pattern is cylindrically symmetric about the z axis. However, because of the in-plane distortion and the relatively large in-plane correlation lengths, the scattering from the two inequivalent sets of peaks [$Q_z = 0$ and $Q_z = \pm(2\pi/c)$] occur at distinct Q_{xy} values [$Q_{xy} = 0.988(4\pi/\sqrt{3}a)$ and $Q_{xy} = 0.955(4\pi/\sqrt{3}a)$, respectively.] Here $c = 30.6$ Å is the effective molecular length and $a = 5.05$ Å is the hexagonal lattice parameter in the CrB phase. Consequently, the powder average produces two distinct concentric cylinders of scattering and the inequivalent peaks can be easily separated. This also enables us to discriminate between the two possible tilted hexatic phases: the SmI and SmF in which the molecular tilt is towards and between nearest neighbors, respectively. The corresponding powder-averaged peaks in the SmF phase would have $Q_z = \pm 1.3(2\pi/c)$ and $Q_z = \pm 2.6(2\pi/c)$. We performed the necessary Q_z scans to establish the Sm I character of the films studied here. In the SmC phase, the scattering is much more diffuse because the in-plane correlation lengths are much smaller, and the powder average produces a diffuse cylinder of scattering. Because of the differences in the scattering patterns in the radial direction, films in the SmI phase, the SmC phase, or a combinations of the two are easily distinguished by the appropriate PSPC scans. Scans along Q_z in the SmI or SmC phase produce patterns consistent with the calculat-

ed molecular form factor, indicating no measurable interlayer correlations.

Representative PSPC scans for films in the different phases are shown in Fig. 2. Figs. 2(a) and 2(b) show PSPC scans for $Q_z=0$ and $Q_z=2(2\pi/c)$ for a five-layer

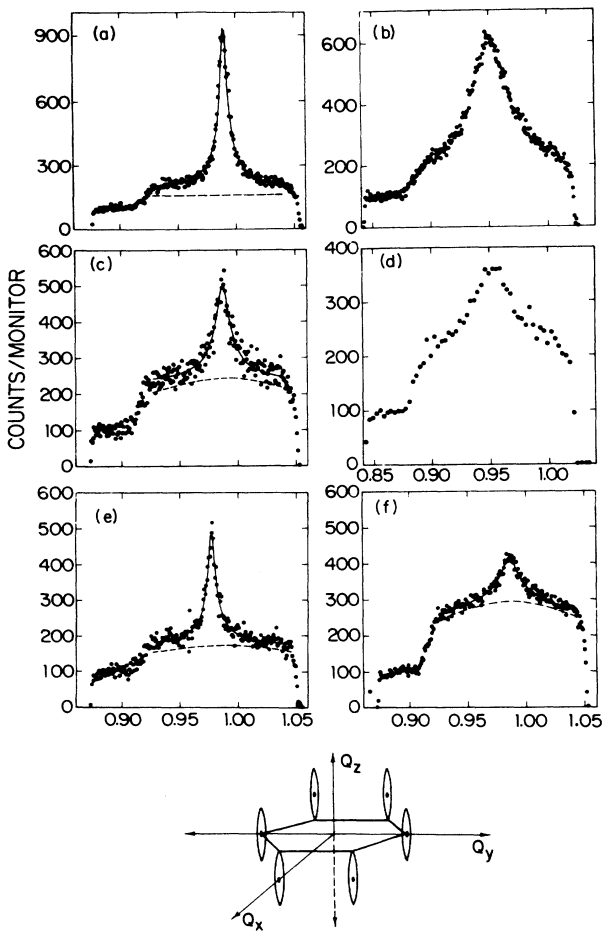

FIG. 2. The inset is a schematic illustration of the SmI scattering peaks. The solid hexagon is in the Q_{xy} plane. The six hexatic scattering rods are shown. There are a pair of peaks centered at $Q_z=2(2\pi/c)$, a pair at $Q_z=0$ and a pair at $Q_z=-2(2\pi/c)$, where $c=30.6$ Å. The plane containing the centers of the hexatic peaks makes an angle of 19.5° to the Q_{xy} plane. The data represent PSPC scans showing SmI and the surface SmI scattering. The solid lines indicate fits to the scattering and background intensities. The dashed lines represent the diffuse component. The units for Q_{xy} are $(4\pi/\sqrt{3}a)$ Å^{-1}, where $a=5.05$ Å. Here N is the number of layers in a film. The monitor provides a measure of the incident flux. (a) The entire film is SmI, $N=5$, $Q_z=0$, $T=66$°C. The fit obtains $\xi=270$ Å. Data was collected for 30 minutes. (b) Same as (a) for $Q_z=2(2\pi/c)$. (c) SmC with SmI on surface, $N=6$, $Q_z=0$, $T=74.0$°C, $\xi=170$ Å. Data was collected for 10 minutes. (d) Same as (c) for $Q_z=2(2\pi/c)$. (e) SmC with SmI on surface, $N=3$, $Q_z=0$, $T=74.0$°C, $\xi=280$ Å. Data was collected for 15 minutes. The surface scattering SmI intensity is the same as for the six-layer film in 1(c). (f) SmC with SmI on surface, $N=6$, $Q_z=0$, $T=76.5$°C, $\xi=130$ Å. Data was collected for 50 minutes. The surface SmI peak is wider than the lower temperature observation in 1(c).

film at 66°C where the film is completely SmI. The anisotropy in the in-plane correlations[9] between the $Q_z=0$ and the $Q_z=\pm2(2\pi/c)$ peaks is very clearly shown in the PSPC scans. The shadowed portion of the detector is clearly visible at low Q_{xy} in Fig. 2(a) between $Q_{xy}=0.87$ and 0.92. The unshadowed portion is between $Q_{xy}=0.93$ and 1.04. Similar regions are visible in Figs. 2(a)—2(f), but the ranges depend on the actual position of the PSPC and are slightly different. The solid lines in Figs. 2(a)—2(f) indicate the fits to the no-film background (shadowed portion) and the peak plus diffuse intensity (unshadowed portion). The fitting is discussed below. Figures 2(c) and 2(d) show PSPC scans for a six-layer film at 74°C where the interior of the film is SmC and the two surface layers are SmI. In these scans, the SmI peaks from the two surface layers are sitting on top of a broad pedestal formed by the much wider SmC scattering ($\xi\sim10$ Å). Because only two surface layers are SmI, the peak intensities in Figs. 2(c) and (d) are considerably weaker than those in Figs. 2(a) and (b) where the film is completely SmI. The six-layer peak in the 74°C scan is slightly broader than that at 66°C, but it is significantly narrower than the SmC peak and is comparable with other hexatics.[9,16,27] The scans in Figs. 2(c) and 2(e) illustrate the fact that the widths vary with film thickness.

To determine the fractions of the film in the SmI and SmC phases, we measured the scattering intensities for 16 films with five different thicknesses. Measurements are presented here for $T=74$°C, 76.5°C, and 77.5°C. After first subtracting the flat no-film background, the resulting PSPC scans (see Fig. 2) were fit to the convolution of the instrumental resolution with a square root Lorentzian (SRL) to represent the peak from the SmI layers: $S(Q_{xy})=A\xi[1+(Q_{xy}-Q_0)^2\xi^2]^{-1/2}$, where Q_0 is the position of the peak and a second SRL to account for the broader diffuse SmC scattering. The SRL form was used because the χ average that results from the 2D powder requires an integration over one of the two dimensions of the 2D hexatic.[16,28] The width of the diffuse peak used in the fitting was that of the underlying SmC peak, as measured by a broad H scan for a six-layer film at 76.5°C. This value, $1/\xi=0.099\pm0.006$ Å, agrees with previously measured widths for the SmC, and with the diffuse widths found from fits where this parameter was allowed to vary. In the above equation for the hexatic line shape, A is constant for a given number of scatterers.

The resulting scattering amplitude A, the product of peak intensity ($A\xi$) and the peak width ($1/\xi$), the peak widths, and diffuse intensity versus film thickness are plotted in Figs. 3(a)—(c). For the films measured, A is essentially independent of thickness and equal to the value for $N=2$, indicating that this scattering comes from the surfaces of the film. The diffuse scattering intensity scales linearly with the film thickness; however, it extrapolates to zero for $N\sim1$, indicating that the diffuse scattering from the SmC layers is stronger than that from the SmI layers. Although incoherent scattering also contributes to the diffuse intensity, no significant incoherent scattering was observed in a broad H scan.

Although we have not studied the pretransitional behavior of the surface hexatic melting in detail, it is clear

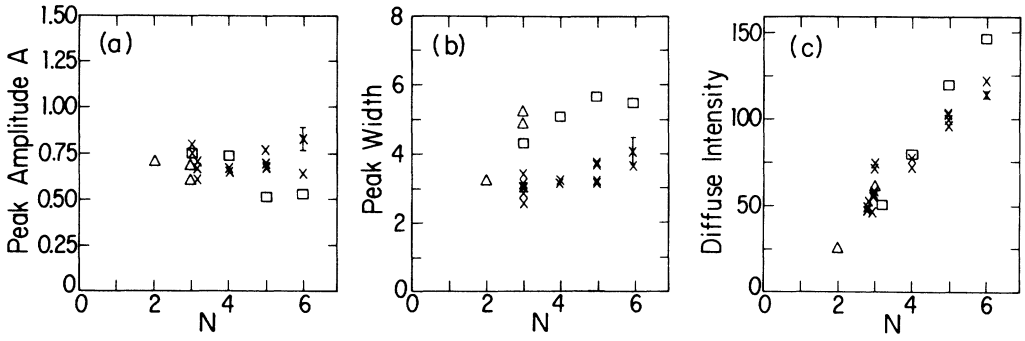

FIG. 3. Results of the fits. Data is presented for $T=74\,^{\circ}\mathrm{C}$ (crosses), 76.5 °C (squares), and 77.5 °C (triangles). Typical error bars are shown for each plot. (a) Scattering amplitude (A) of the SmI surface peaks at $Q_z=0$. The data indicate that the surface SmI peak scattering is roughly independent of both film thickness and temperature. Units are counts $\times(4\pi/\sqrt{3}a)$/ monitor. (b) Peak widths ($1/\xi$) vs number of layers. Surface SmI correlation lengths decrease with increasing N and with increasing temperature. Units are $10^{-3}(4\pi/\sqrt{3}a)$. (c) The diffuse scattering intensity underneath the $Q_z=0$ peaks as a function of film thickness. This intensity is partly from the SmC interior and partly from the diffuse scattering of the SmI layers. Units are counts/monitor.

that at higher temperatures the SmI surface peaks broaden, indicating shorter hexatic correlation lengths. At $\sim 78\,^{\circ}\mathrm{C}$ the SmI peaks disappear, indicating the melting of the surface hexatic layers into the SmC phase. For two-layer films the SmC to SmI transition occurs $\geq 1\,^{\circ}\mathrm{C}$ higher than the surface transition in the thicker films.

CONCLUSIONS

In summary, we have shown that there are monolayer surface hexatic layers on the two exterior surfaces of SmC films of 7O.7 between 69 °C and $\sim 78\,^{\circ}\mathrm{C}$. These surface layers have the two-dimensional structural properties of the SmI phase that is observed below $\sim 69\,^{\circ}\mathrm{C}$ for films thinner than ~ 20 layers. The melting of the hexatic surface layers has not yet been characterized in detail but may be very interesting because it represents the novel case of a tilted hexatic monolayer on a tilted liquid substrate. A pretransitional broadening of the SmI surface peaks is observed before melting. The transition from the hexatic surface SmI phase to the homogeneous SmI phase below 69 °C has also not been studied in detail, and it should also be interesting to study the development of strong hexatic-SmI order in the interior SmC layers which should occur at this transition. Finally, from a technical point of view, these measurements clearly demonstrate the utility of parallel detection techniques in synchrotron x-ray scattering studies of weakly scattering systems.

ACKNOWLEDGMENTS

We wish to acknowledge useful conversations with Allan Farber. We also wish to thank the entire SSRL staff for their help. This work was supported by the National Science Foundation under Grants No. NSF-DMR-82-12189 and No. NSF-DMR-83-16979. Part of this work was done at the Stanford Synchrotron Radiation Laboratory, which is supported by the U.S. Department of Energy (Office of Basic Energy Sciences).

[1]K. Binder, in *Phase Transitions and Critical Phenomena,* edited by C. Domb and J. L. Lebowitz (Academic, New York, 1983), Vol. 8, p. 1.

[2]D. R. Nelson, in *Phase Transitions and Critical Phenomenon,* edited by C. Domb and J. L. Lebowitz (Academic, New York, 1983), Vol. 7.

[3]Douglas Sluis and Stuart A. Rice, J. Chem. Phys. **79**, 5658 (1983).

[4]M. P. D'Evelyn and S. A. Rice, Phys. Rev. Lett. **47**, 1844 (1981).

[5]J. Als-Nielsen, F. Christensen, and P. S. Pershan, Phys. Rev. Lett. **48**, 1107 (1982).

[6]K. Miyano, Phys. Rev. Lett. **43**, 51 (1979).

[7]D. J. Bishop, W. O. Sprenger, R. Pindak, and M. E. Neubert, Phys. Rev. Lett. **49**, 1861 (1982).

[8]D. E. Moncton, R. Pindak, S. C. Davey, and G. S. Brown, Phys. Rev. Lett. **49**,, 1865 (1982).

[9]E. B. Sirota, P. S. Pershan, L. B. Sorensen, and J. Collett, Phys. Rev. Lett. **55**, 2039 (1985).

[10]S. Heinekamp, Robert A. Pelcovits, E. Fontes, E. Yi Chen, R. Pindak, and R. B. Meyer, Phys. Rev. Lett. **52**, 1017 (1984).

[11]J. M. Kosterlitz and D. J. Thouless, J. Phys. C **6**, 1181 (1973).

[12]B. I. Halperin and D. R. Nelson, Phys. Rev. Lett. **41**, 121 (1978).

[13]A. P. Young, Phys. Rev. B **19**, 1855 (1979).

[14]S. E. Nagler, P. M. Horn T. F. Rosenbaum, R. J. Birgeneau, M. Sutton, S. G. J. Mochrie, D. E. Moncton, and R. Clarke, Phys. Rev. B **32**, 7373 (1985).

[15]R. Pindak, D. E. Moncton, J. W. Goodby, and S. C. Davey, Phys. Rev. Lett. **46**, 1135 (1981).

[16]S. C. Davey, J. Budai, J. W. Goodby, R. Pindak, and D. E. Moncton, Phys. Rev. Lett. **53**, 2129 (1984).

[17]J. Collett, P. S. Pershan, E. B. Sirota, and L. B. Sorensen, Phys. Rev. Lett. **52**, 356 (1984).
[18]D. J. Bishop and J. D. Reppy, Phys. Rev. B **22**, 5171 (1980).
[19]J. Collett, L. B. Sorensen, P. S. Pershan, R. J. Birgeneau, J. D. Litster, and J. Als-Nielsen, Phys. Rev. Lett. **49**, 553 (1982).
[20]J. P. Hirth, P. S. Pershan, J. Collett, E. B. Sirota, and L. B. Sorensen, Phys. Rev. Lett. **53**, 473 (1984).
[21]Jeffrey Collett, L. B. Sorensen, P. S. Pershan, and J. Als-Nielsen, Phys. Rev. A **32**, 1036 (1985).
[22]A. J. Leadbetter, M. A. Mazid, B. A. Kelly, J. W. Goodby, and G. W. Gray, Phys. Rev. Lett. **43**, 630 (1979).
[23]Allan S. Farber, PhD. thesis, Brandeis University, 1985.
[24]P. A. C. Gane, A. J. Leadbetter, and P. G. Wrighton, Mol. Cryst. Liq. Cryst. **66**, 245 (1981).
[25]J. J. Benattar, F. Moussa, M. Lambert, and C. Germain, J. Phys. (Paris) Lett. **42**, 67 (1981).
[26]J. Doucet, P. Keller, A. M. Levelut, and P. Porquet, J. Phys. (Paris) **39**, 548 (1978).
[27]J. J. Benattar, F. Moussa, and M. Lambert, J. Chem. Phys. **80**, 99 (1983).
[28]B. M. Ocko, A. R. Kortan, R. J. Birgeneau, and J. W. Goodby, J. Phys. (Paris) **45**, 113 (1984).